Synergistic effects of COF and GO on high flux oil/water separation performance of superhydrophobic composites

Han Wang[a], Mengke Wang[b], Yanling Wang[c], Jing Wang[a], Xuehu Men[a*], Zhaozhu Zhang[c*], Vikramjeet Singh[d*]

[a] *Key Laboratory for Magnetism and Magnetic Materials of the Ministry of Education, School of Physical Science and Technology, Lanzhou University, Lanzhou, 730000, P. R. China*

[b] *College of Chemistry and Chemical Engineering, Nantong University, Nantong, 9 Seyuan Road, Nantong, Jiangsu, P. R. China*

[c] *State Key Laboratory of Solid Lubrication, Lanzhou Institute of Chemical Physics, Chinese Academy of Sciences, Lanzhou, 730000, P. R. China*

[d] *Nanoengineered Systems Laboratory, UCL Mechanical Engineering, University College London, London, UK*

Abstract: Covalent organic frameworks (COFs) have been emerged as potential membrane material because of their rigid porous structure and excellent chemical stability, however, the challenges of complicated preparation process and poor processability remain. In this study, a simple one-step method is developed to prepare hybrid composite material from COFs and graphene oxide (GO) without using any special device generally required for COFs fabrication. The under-water stability of GO was enhanced through hybridization with COFs. The hybrid composite formed by

---

* Corresponding author. Tel: +86 931 8912719

E-mail address: menxh@lzu.edu.cn (X. H. Men); zzzhang@licp.cas.cn (Z.Z. Zhang); vikramjeet.singh@ucl.ac.uk (V. Singh)

COF polymerization and parallel covalent linking to the GO in a single step was translated into superhydrophobic and recyclable membrane by spraying onto filter paper. The role of graphene oxide as catalyst/catalyst carrier has been identified in the easy fabrication of COFs in this study. The fabricated membrane presented ultra-high separation flux of 26000 L m^{-2} h^{-1} bar^{-1} with >98% separation efficiency. The membrane exhibited exceptional chemical stability in acid and basic environment with excellent cycling stability. A simple methodology presented here opens up a new route for the fabrication of COF based hybrid materials for wide range of applications.

1. Introduction

Covalent organic frameworks (COFs), a new class of porous polymeric material which comprises of two organic monomers linked through highly stable covalent bond have been identified as promising membrane material with excellent performance due to various structural advantages.[1-3] Robust customized structure and precise control over the functionality make them dominant when compared with other traditional porous materials such as zeolites and metal-organic frameworks.[4, 5] COFs have been uniquely designed and explored for various applications such as gas and energy storage, separation, sensing, catalysis and drug delivery etc.[6-10] Particularly, the membrane-separation applications attracted much attention due to highly ordered molecular arrangements and robust structure of COFs[ref]. Han's group have fabricated COF-DhaTab blended PAN membrane by electrostatic spinning for oil/water

emulsions separation.[11] Li's team have successfully obtained the stainless-steel-net-supported COF coating for oil/water separation.[12] Recently, attempts have been made to overcome the poor processability of the COFs powder and to translate them into membranes for separation applications.[13-18] Mixing the COFs with graphene/graphene oxide to generate hybrid material is one of the successful attempt that researchers are currently exploring.[19-21]

Graphene/graphene oxide is also a widely researched material for their applications as desalination and separation membranes due to its excellent mechanical and thermal strength, large surface area and ease of 2D sheet formation.[22-24] Nevertheless, the use of graphene in oil/water separation is limited by its poor stability caused by increase in interlayer spacing distance between sheets in water due to weak π-π interactions.[25-27] Therefore, hybrid composites have been prepared by mixing graphene with COFs and other polymers to improve the overall stability.[28, 29]

Khan's team has fabricated GO-CTF mixed nanosheet membranes with high rejections capabilities to organic dyes.[30] Zhang and his co-workers have obtained GO/COF-1 nanosheets membrane with high rejection rate for water soluble dyes and high permeability for ion salts.[31] However, the obtained water flux of the membrane is only 310 L m^{-2} h^{-1}MPa^{-1}. Jiang's group have successfully prepared v-COF@GO membranes for oil/water separation, but the material needs to be further sulfonated to change wettability, in addition, the experimental process is rather complicated and laborious.[32]

In this work, a one-step method is developed to produce COF/GO hybrid material

without using any special equipment. Highly stable hydrophobic COFs, Ⅱ SERP-COF2-β were grown on graphene nanosheets through the formation of amide bonds and parallel Schiff base reaction. The resulting COF/GO membrane possesses superhydrophobicity with water contact angle (WCA) up to ~160° without the need of any post-synthetic modification using low energy molecules as required in previous reports. Owing to the synergistic effect with graphene, the agglomeration of COFs materials is significantly reduced and on the other hand, structural and chemical stability of the graphene is also improved due to the acid and alkali resistance of COFs. The overall pore size of the hybrid material is increased in comparison with GO which resulted into decrease in the oil resistance. The flux of separating water/dichloromethane mixture is recorded as high as 26000 L m^{-2} h^{-1} bar^{-1}. Additionally, the membrane exhibits excellent acid/base resistance, high separation flux for the water (pH=1 and 13) and n-hexane mixtures and high separation efficiency.

2. Experimental section

2.1 Materials

Graphite powder, P-phenylenediamine, acetic acid and sulfuric acid were purchased from Shanghai Macklin Biochemical Co. N,N-dimethylformamide, potassium persulfate were obtained from Fengchuan Chemical Reagent Co. (Tianjin,China). Phosphorus pentoxide, o-dichlorobenzene, hydrogen peroxide, hydrochloric acid, potassium permanganate and toluene were supplied from Kemiou Chemical Reagent Co .(Tianjin,China). Ethanol, acetone, hexane, dichloromethane, chloroform and span

80 were provided from Shuangshuang Chemical Reagent Co. (Yantai, China). All reagents were used without further purification.

2.2 Characterization

The morphologies of the GO and COF/GO_X were characterized by scanning electron microscope (SEM, Apreo S) and transmission electron microscopy (TEM, FEI Tecnai F30, 300 kV).The chemical structure of the samples were carried out by Fourier transform infrared spectrometer (FTIR, Bruker,Tensor 27). The chemical composition of C and N elements was obtained by X-ray photoelectron spectroscopy (XPS, Kartos AXIS Ultra DLD, with Al Kα X-ray source, hv = 1486.6 eV).The X-ray diffraction (XRD, Philip X'Pert pro Diffractometer, with Cu Kα X-ray source, λ = 1.54056 Å) was obtained at room temperature. The WCAs of GO and COF/GO_X were measured using 5 μL droplets by an optical contact angle measuring apparatus (JGW-360B) at room temperature. The Raman (HORIBA Jobin Yvon LabRAM HR800) shifts were characterized using a 532 nm YAG laser with a laser spot diameter of ~600 nm. The nitrogen adsorption-desorption curves and pore size distribution curves of samples were measured by surface area and porosity analyzer (Micromeritics ASAP 2020 HD88, 77 K). The thermal stability of the GO and COF/GO_x were measured by thermogravimetric (TGA) analyzer (NETZSCH STA 449F3, 10.0°C /min, 20 °C ~800 °C , air atmosphere).

2.3 Synthesis of Tris(4-formylphenyl)amine

The preparation of Tris(4-formylphenyl)amine was referred to Dinesh Mullangi's work.[33] In brief, phosphorus oxychloride was added drop wise to the

dimethylformamide (DMF) at 0 °C in Ar, the mixtures stirred to melt at room temperature for about 1 h, then triphenylamine and chloroform were added to the above-mentioned mixtures at 80 °C under continuous stirring for 12 h. After cooling down, the solution was poured into ice water and pH was adjusted to 7 using diluted NaOH solution (3 M). After extraction with dichloromethane, the organic layer was washed with salt solution and water for three times, then it was dried with Na_2SO_4 granule and the solvent was removed through vacuum distillation. The residue was filtered through a short column with a mixture of n-hexane/dichloromethane to obtain a yellow solid which was then added to the solution of phosphorus oxychloride and DMF at 80 °C for 12 h, the obtained mixture was poured into ice water, and repeated the above steps to obtain yellow crystalline compound, tris(4-formylphenyl)amine.

2.4 Synthesis of graphene oxide

Graphene oxide was reduced according to the modified Hummers method in brief, $K_2S_2O_8$ (5 g) and P_2O_5 (5 g) were dissolved in concentrated sulfuric acid for 12 h under stirring, then graphite flakes were added, and the mixture was kept in an oil bath at 90 °C for 5 h. The mixture was diluted with 800 mL of deionized water after cooled down to room temperature to obtain expanded graphite, and dried powder at 60 °C for 12 h. Next, expanded graphite and $KMnO_4$ were added to 100 ml of concentrated sulfuric acid under stirring, followed by 12 h in an oil bath at 35 °C. The obtained solution was poured into 600 mL of deionized water in an ice bath, and H_2O_2 was slowly dropped into the mixture. After standing for 10 h, the precipitate was washed with 10% hydrochloric acid and deionized water until it was close to neutral.

Finally, the precipitate was freeze dried to obtain GO powder.

2.5 Synthesis of COF/GO$_x$ powders and COF/GO$_x$ membranes

Tris(4-formylphenyl)amine (200 mg) and P-phenylenediamine (100 mg) were dissolved in ethanol (15 mL) under magnetic stirring for 20 minutes, then the o-dichlorobenzene (15 mL) was dropped slowly until the mixture becomes yellow and transparent. Next, acetic acid (1.25 mL) and graphene oxide were added in sequence under stirring for 5 minutes. Then the solution was transferred into a quartz tube, after sealing in liquid nitrogen bath, the quartz tube was placed in an oven and kept at 120 °C for 3 days. The obtained precipitates were washed with DMF and acetone three times and dried at 60 °C for 4h to obtain COF/GO$_x$, where x = 25, 50,75 and 100 which represents the mass of graphene oxide which was 25 mg, 50 mg, 75 mg and 100 mg, respectively. A series of samples were prepared to explore the effect of graphene proportion in the membrane.

0.3 g COF/GO$_x$ was dissolved in 15mL ethyl acetate. Then the solution was sprayed onto filter paper using a spray gun with 0.2 MPa spraying pressure and a moving speed of 3–5 cm/s. The distance between the spray gun and the filter paper was 15–20 cm during spraying. Finally, the obtained COF/GOx membranes were placed in oven at 50 °C for 1 h. The preparation steps of GO membrane was similar.

2.6 Separation of oil/water mixtures

Organic solvents (hexane, dichloromethane, chloroform and toluene) were used as oil in oil/water separation process. The equivalent of 10 mL water and 10 mL oil were poured into sand core device for oil/water separation with COF/GO$_{50}$ membrane

under 0.67 bar. The oil samples passed through the device and were collected in the bottle. The flux was calculated by the following equation:

$$J=\frac{V_1+V_2}{S{\cdot}t{\cdot}P}$$

(1)

where V_1 and V_2 were the volume of water and oils samples, respectively. S was the effective area of oil passing through the membrane, t was the time of oil permeation and P was the pressure applied to the separation device which is 0.67 bar.

The separation efficiency was calculated by following equation:

$$\eta=\frac{V_2}{V_3} \times 100\%$$

(2)

where V_3 was the volume of oil collected in the bottle. In the oil/water separation cycles test, the membrane was not pretreated and was used continuously.

3. **Results and discussion**

3.1 Single step fabrication of COF/GO composites and role of graphene in catalysis enhancement
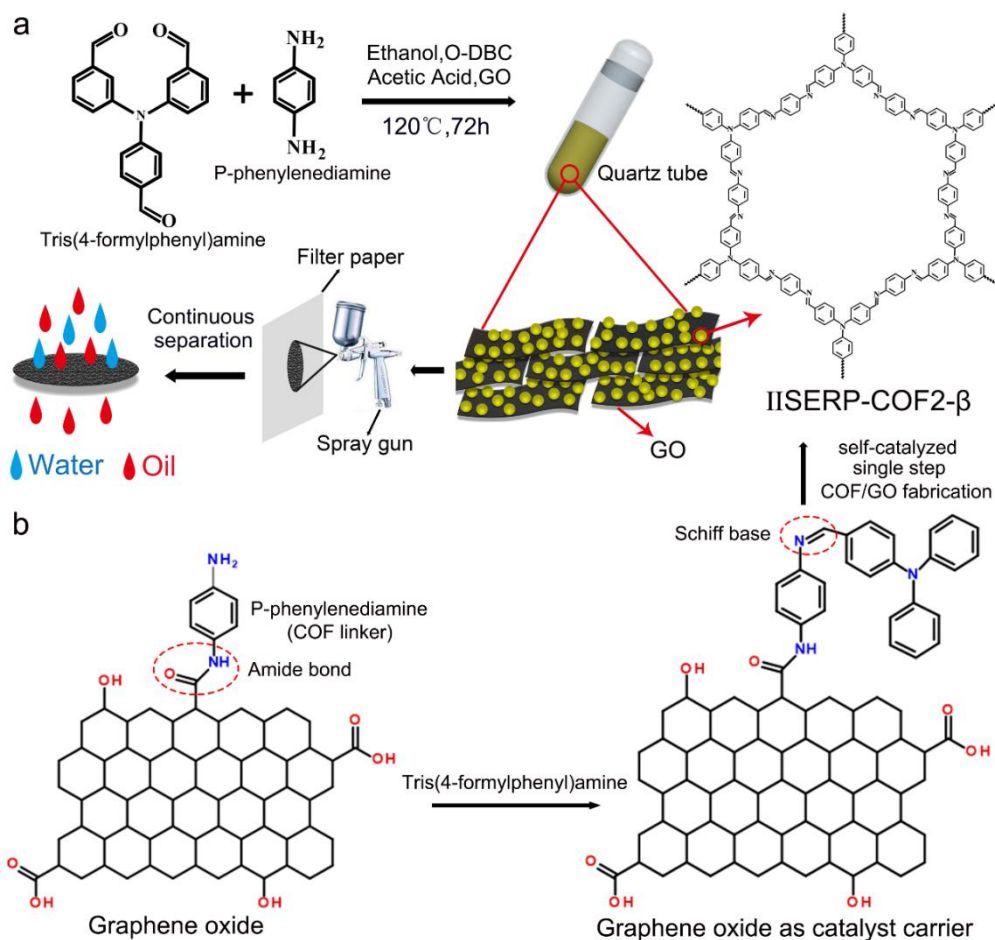
Figure 1. (a) Schematic showing the one-step fabrication method for COF/GO$_x$ composition followed by membrane preparation via spraying the composite onto the filter paper. And (b) the growth mechanism of COF on the GO sheets at the molecular level and the role of grapheme oxide as Schiff base carrier.

An ordinary quartz tube is used instead of microwave reactor or special Pyrex heat-resistant glass tube which is generally required for the preparation of COFs (Figure 1a). In addition, the freeze-pump-thaw cycles and the use of acetylene-oxygen flame to seal the bottle under vacuum were also avoided. COF particles were successfully grown on graphene sheets under ambient temperature condition. As

prepared material was translated into free standing membrane by simply spraying it on the filter paper that presents cost effective sustainable approach. The growth mechanism of COF on GO nanosheets is presented in Figure 1b. One of the amine group presented on P-phenylenediamine reacts with the carboxyl group on GO to form an amide bond, while another one reacts with the carbonyl group of Tris(4-formylphenyl) amine by Schiff base reaction in a continuous process results into COF/GO composite. The graphene oxide acted as Schiff base (Ph-N=C-Ph) carrier in reaction which could possibly contributed in the easy fabrication of COFs. The role of graphene oxide as a catalyst carrier and/or itself as a catalyst is well understood.[34-36] As a proof to confirm the role of graphene oxide in our study, a COF fabrication reaction without GO has been setup as a control and no precipitation of COFs has been observed. However, under similar condition, the COFs could be successfully synthesized with the addition of GO regardless of concentration which confirmed the direct role of the GO in the catalysis enhancement.
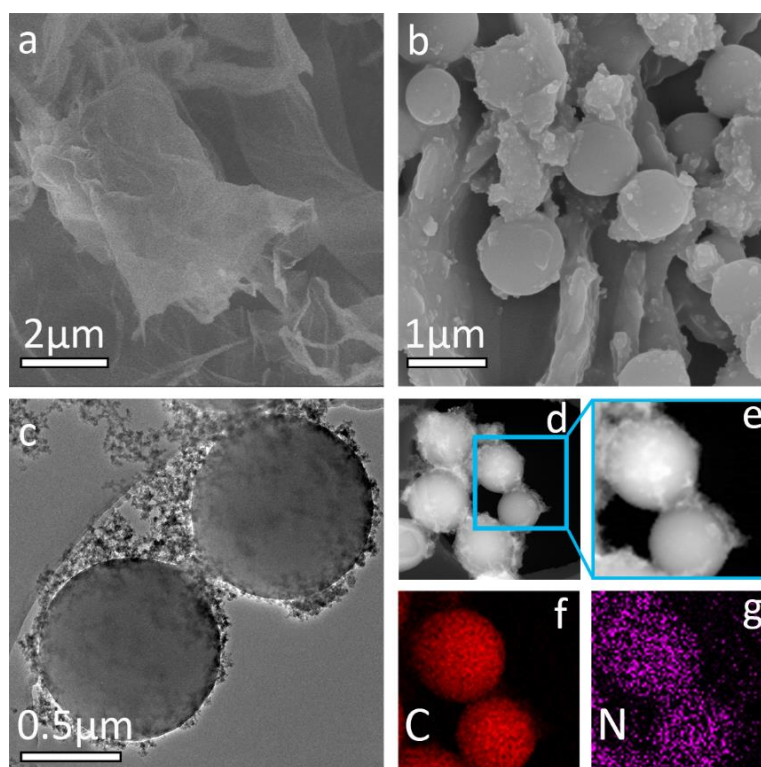
Figure 2. (a) SEM image of GO. (b) SEM image of COF/GO$_{50}$. (c) - (e) TEM images of

COF/GO$_{50}$. (f) - (g) EDS mapping of COF particles.

Morphology of GO sheets showing wrinkled structure was recorded by SEM is shown

in Figure 2a. Figure 2b is showing the morphology of COF/GO$_{50}$ hybrid composite

where the spherical COF particles with 0.6-1 µm size could be clearly observed.

Figure 2c and 2e showing the TEM images of COF/GO$_{50}$, in which COF particles

exhibit homogeneous spherical shape and are covered with GO sheets. Figure 2f and

2g showing the elemental distributions of C and N, respectively. C and N elements are

shown to be evenly distributed on the COF sphere, which constitute the basic
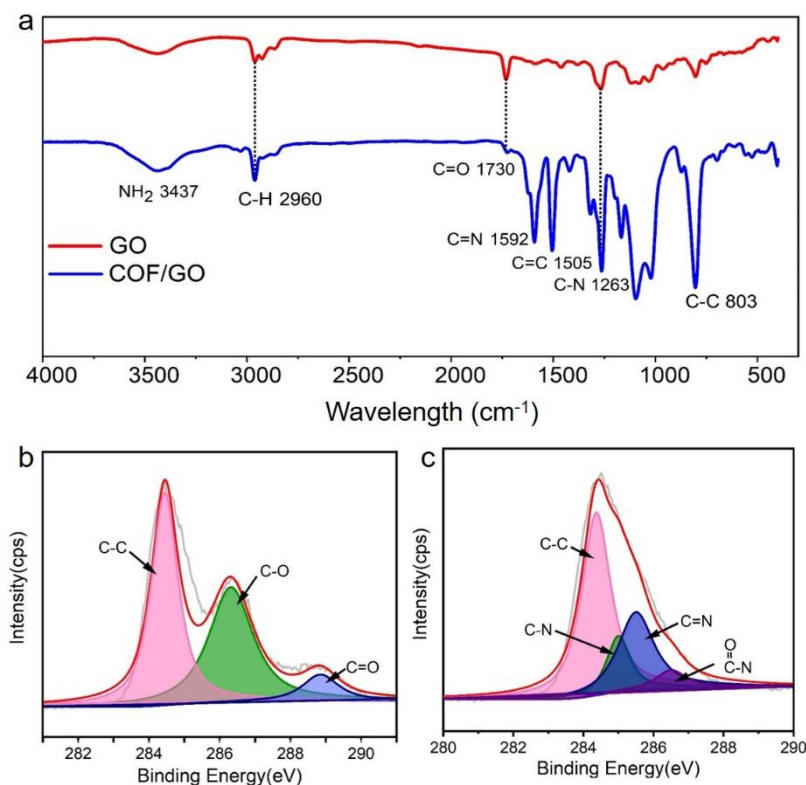
chemical frameworks of the COFs.

Figure 3. (a) FTIR spectra of GO, GO and COF/GO$_{50}$. (b) - (c) C 1s XPS of GO and COF/GO$_{50}$, respectively.

FTIR spectra of GO and COF/GO$_{50}$ have been recorded for the structural confirmation (Figure 3a). Characteristic peak at 1505 cm^{-1} represents the stretching vibration of phenyl ring of COF particles in COF/GO$_{50}$ composite. The intensity of peak at 1730 cm^{-1} has been reduced significantly in COF/GO$_{50}$, indicating the utilization of carboxyl group. In addition, the obvious peak at 1263 cm^{-1} for C-N is also appeared. The above results confirmed the covalent linkage between COFs and graphene. The peak at 1592 cm^{-1} could be attributed to C=N in the spectra, which confirmed the successful synthesis of COF particles.

To further confirm the chemical structure of COFs particles on GO sheets and connection between COF and GO sheets, GO and COF/GO$_{50}$ were analyzed by XPS.

Three peaks at 284.5, 286.6 and 288.4 eV could be attributed to C-C, C-O and C=O bonds in GO, respectively. The C 1s spectrum of COF/GO$_{50}$ in Figure 3c exhibited four peaks at 284.5, 284.9, 285.5 and 286.5 eV for C-C, C-N, C=N and O=C-N bonds, respectively. Both, XPS and FITR spectra illustrated the successful synthesis of COF materials and the covalent bonds formation between COF particles and GO sheets.
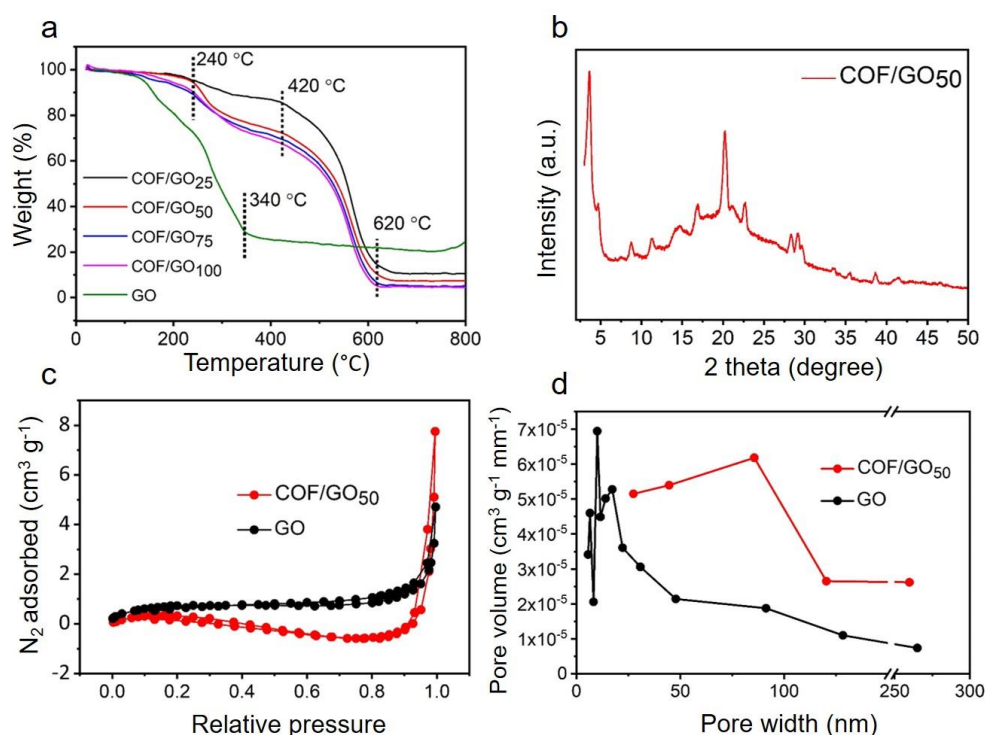

Figure 4. Physicochemical characterization of COF/GO (a) TGA analysis curves of COF/GO$_x$ and GO. (b) XRD pattern of COF/GO$_{50}$. (c) Nitrogen adsorption-desorption curves of COF/GO$_{50}$ and GO. (d) Pore size distribution of COF/GO$_{50}$ and GO.

The obtained TGA curves of COF/GO$_X$ samples and GO are presented in Figure 4a. The temperature range from 240 to 420 °C could be attributed to the graphene degradation where the height of each curve decreased at different rates. Decomposition of COFs could be observed at 420-620 °C. The hybrid composite

showed enhanced thermal stability when compared to that of GO might be due to the stability reinforcement by covalent bonding. The slower decomposition of COF/GO$_{25}$ when compared with other ratios could also be explained by the higher content of COFs. The crystallinity of the COFs in COF/GO$_{50}$ composite was confirmed by two characteristic peaks at 3.6º and 4.7º in PXRD spectra which are in complete agreement with the previous studies.[33] The nitrogen adsorption-desorption curves of COF/GO$_{50}$ and GO in Figure 4c indicating the presence of H4 type hysteresis rings and hence the existence of nanopores in both, COF/GO$_{50}$ and GO. The high nitrogen adsorption capacity of COF/GO$_{50}$ at relative pressure >0.9 suggesting the existence of larger pores in COF/GO$_{50}$ composite. Overall, the COF/GO$_{50}$ and GO exhibited multi-level pore structure and the proportion of micropores in COF/GO$_{50}$ was recorded to be much larger than GO (Fig. 4d).
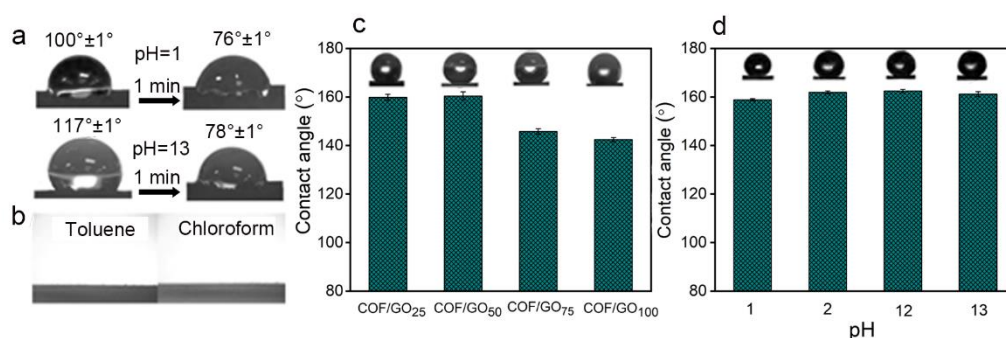
3.2 Wettability of COF/GO$_x$ and GO membranes

Figure 5. (a)WCAs of water with acidic (pH=1) and basic (pH=13) pH on GO membrane. (b) Images of toluene and chloroform drops on the COF/GO$_{50}$ membrane showing complete wettability. (c) Change in the WCAs with GO proportions in COF/GO membranes. (d) WCAs on COF/GO$_{50}$ membrane with different acidic and basic pH. The droplets were placed for ~2 minutes and no change in the angles have

been recorded.

The stability of GO membrane is tested under acidic and basic conditions for comparison and the data is presented in Figure 5a. Static contact angle of acidic (pH=1) and basic (pH=13) solution droplets was dramatically decreased from 100° to 76° and 117° to 78°, respectively just after one minute of exposure due to poor stability of GO membrane under acidic/basic conditions. Toluene and chloroform were absorbed instantaneously after being dropped on the COF/GO_{50} membrane indicated the superoleophilic nature of the membrane (Figure 5b). As shown in Figure 5c, the WCAs of membranes with smaller proportions of GO, COF/GO_{25} and COF/GO_{50} were recorded >160°, whereas WCAs of COF/GO_{75} and COF/GO_{100} combinations were found to be ~150°, might be due to decrease in the roughness where COFs particles have contributed. The roughness of COF particles grown on GO sheets and the inherited hydrophobic nature of graphene synergistically contributed in the superhydrophobicity. Considering the wettability, COF content and cost effectiveness, COF/GO_{50} membrane is selected to further evaluate the oil/water separation efficiency. In real-world applications of superhydrophobic materials, their stability under the harsh acid and alkali environment is extremely important. Therefore, WCAs on COF/GO_{50} membrane at different pH, 1, 2, 12 and 13 have been measured and the data is presented in Figure 5d. The membrane maintained its superhydrophobicity regardless of pH (acidic and basic) with WCA recorded to be >155° which confirmed the excellent stability of the membrane.
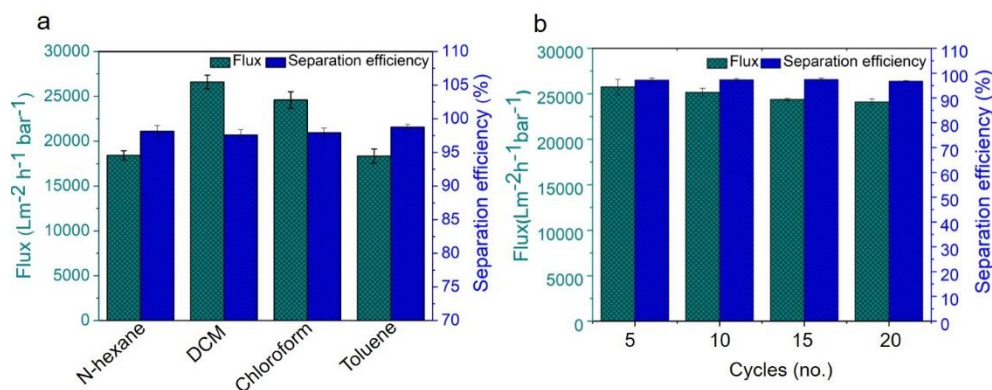
3.3 Oil/water separation performance of COF/GO$_{50}$ membrane

Figure 6. Separation performance of COF/GO$_{50}$ membrane (a) Flux and separation efficiency of four types water/oil mixtures. (b) Flux and separation efficiency during 20 repeated cycles of water/dichloromethane mixture.

Oil/water separation performance of the COF/GO$_{50}$ membrane is presented in Figure 6a. The measured membrane fluxes for separating n-hexane, dichloromethane, chloroform and toluene from water were 18412 Lm^{-2}h^{-1} bar^{-1}, 26960 Lm^{-2}h^{-1} bar^{-1}, 23590 L m^{-2}h^{-1} bar^{-1} and 18942 L m^{-2}h^{-1} bar^{-1}, respectively. At the same time, the separation efficiency was recorded 98.9%, 99.3%, 98.3% and 99.2%, respectively. The high flux could be explained with the increase in the large pore volume proportion of material after combining GO with COFs which significantly enhanced the oil permeability of the membrane. Meanwhile, part of oil directly passed through the COF particles instead of flowing between the narrow layers of GO, which significantly reduced the hindrance. The separation efficiency of the membrane was further evaluated by 20 repeated separation cycles of water and dichloromethane mixture without any treatment or in between washing. As shown in Figure 7b, the

separation flux was slightly decreased from 26000 L m^{-2} h^{-1} bar^{-1} to 24000 L m^{-2} h^{-1} bar^{-1} after 20 repeated cycles might be due to the temporary blockage of the pores. However, the overall flux rate remained high and membrane also maintained the high separation efficiency of 98.5% after 20 cycles.
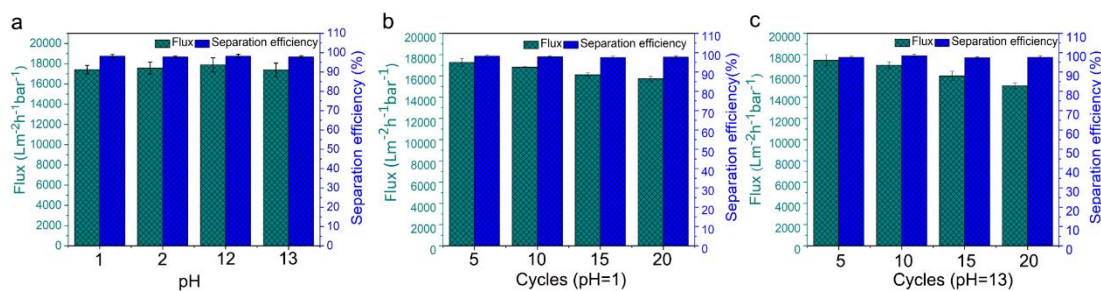

Figure 7. Separation performance of COF/GO$_{50}$ membrane under adverse conditions (a) Flux and separation efficiency of different pH water/oil mixtures. (b) Flux and separation efficiency during 20 cycles of water (pH=1)/n-hexane mixture. (c) Flux and separation efficiency during 20 cycles of water (pH=13)/n-hexane mixture.

The oil/water separation efficiency of the developed membrane was also tested under severe acidic (pH=1 and 2) and basic (pH=12 and13) environments. Mixture of n-hexane and water with different pH was prepared and used for testing and the obtained results are shown in Figure 7a. For acidic pH of 1 and 2, the separation fluxes were recorded 17400 L m^{-2} h^{-1} bar^{-1} and 17570 L m^{-2} h^{-1} bar^{-1}, and the separation efficiencies were 98.2% and 98.0%, respectively. Whilst for the alkaline pH of 12 and 13, the separation fluxes were recorded 17800 L m^{-2} h^{-1} bar^{-1} and 17380 L m^{-2} h^{-1} bar^{-1}, and the separation efficiencies were 98.3% and 98.0%, respectively. The COF/GO$_{50}$ membrane successfully maintained its separation efficiency above 98% and only slight decrement in the separation flux was recorded when compared with

that obtained from neutral water and n-hexane mixture (18412 L m^{-2} h^{-1} bar^{-1}). This clearly shows the enhanced performance of the hybrid composite due to the inherent acid and basic resistance of COFs over traditional GO membranes.

Table 1. State-of-the-art comparison with the presented work for oil/water separation performance.

Materials	Efficiency (%)	Flux ($Lm^{-2}h^{1}$)	Pressure	Cycles	Acid/base tolerance test	Ref.
SIPN-Gels	>99	8600	Gravity	50	No cycles	[37]
PCLc membrane	>99	2850 - 3560	Gravity	10	No cycles	[38]
Cu(OH)$_2$ mesh	>97	1980	Gravity	20	—	[39]
Cu-MOF	>99	701.71	Gravity	8	—	[40]
PAM/PS membrane	—	—	0.01MPa	20	—	[41]
ZIF-8@nickel mesh	>99	—	Gravity	6	—	[42]
DTMS@WO$_3$ copper mesh	>98	7657 - 9962	Gravity	10	—	[43]
PDMS/ZIF-8@cotton fabric	>98	—	Gravity	10	—	[44]
PDVB/TiO$_2$ composite	—	55 - 70	Gravity	—	—	[45]
PLA materials	—	35 - 50	Gravity	10	—	[46]
COF/GO membrane	>98.3	15100 - 26960	0.67 bar	20	20 cycles	This work

— Not Mentioned

The stability and efficiency of the membrane for 20 repeated cycles of oil/water

separation was also tested at elevated conditions of pH 1 and 13. At pH 1, the separation flux and separation efficiencies of the membrane were slightly decreased from 17300 L $m^{-2} h^{-1} bar^{-1}$ to 15700 L $m^{-2} h^{-1} bar^{-1}$, and 98.3% to 97.85%, respectively. At pH 13, the separation flux and separation efficiencies of the membrane were also slightly decreased from 17400 L $m^{-2} h^{-1} bar^{-1}$ to 15100 L $m^{-2} h^{-1} bar^{-1}$ and 98.5% to 97.7%, respectively. The decrease in the separation flux and separation efficiency might be attributed to the combinatorial effects of temporary pore blockage and acid/base intolerance of GO. Nevertheless, the membrane possessed high separation flux and cycle stability for oil/water separation under severe acid and basic conditions.

Conclusion

In conclusion, a cost effective and rapid method is demonstrated to fabricate and then translate the covalently linked hybrid composite of COFs and graphene into membrane. The role of graphene in catalysis enhancement of COFs fabrication reaction has been identified. The swelling, structural collapse of GO in water and the agglomeration of COFs were significantly reduced due to hybridization of GO and COFs. The obtained COF/GO_x membranes were superhydrophobic without any post-synthetic modification of the material. The COF/GO_{50} membrane showed an ultra-high separation flux of 26000 L $m^{-2} h^{-1} bar^{-1}$ for oil/water separation which is the highest when compared with state-of-the-art COF membranes. The membrane also demonstrated excellent stability at elevated acidic (pH-1) and basic (pH-13) environments by maintaining high flux rate and separation efficiency. Our study

provides new potential ideas for the applications of two promising materials, COFs and graphene in oil/water separation.

Supporting Information

The Supporting Information is available free of charge online.

Preparation of Graphene Oxide, SEM images of COF/GO$_x$, EDS mappings of COF/GO$_{50}$, XRD pattern of GO, XPS spectra of COF/GO$_{50}$ and GO, WCAs of COF/GO$_{50}$ at different pH (3~11).

Separation of water and dichloromethane mixture at 0.67 bar. **(Video S1)**

Notes

The authors declare no competing financial interest.

Acknowledgement

References

(1). D. G. Barnes；M. Vidiassov；B. Ruthensteiner；C. J. Fluke；M. R. Quayle；C. R. McHenry. Embedding and publishing interactive, 3-dimensional, scientific figures in Portable Document Format (PDF) files. *PLoS One*. **2013**, *8*, e69446.

(2). A. P. Cote；A. I. Benin；N. W. Ockwig；M. O'Keeffe；A. J. Matzger；O. M. Yaghi. Porous, crystalline, covalent organic frameworks. *Science*. **2005**, *310*, 1166-1170.

(3). S.-Y. Ding；W. Wang. Covalent organic frameworks (COFs): from design to applications. *Chem. Soc. Rev.* **2013**, *42*, 548-568.

(4). S.-Y. Ding；J. Gao；Q. Wang；Y. Zhang；W.-G. Song；C.-Y. Su；W. Wang. Construction of Covalent Organic Framework for Catalysis: Pd/COF-LZU1 in Suzuki–Miyaura Coupling Reaction. *Journal of the American Chemical Society*. **2011**, *133*, 19816-19822.

(5). X. Feng；X. Ding；D. Jiang. Covalent organic frameworks. *Chemical Society Reviews*. **2012**, *41*,

(6). S. S. Han；H. Furukawa；O. M. Yaghi；W. A. Goddard, 3rd. Covalent organic frameworks as exceptional hydrogen storage materials. *J Am Chem Soc*. **2008**, *130*, 11580-11581.

(7). H. Jin；C. Guo；X. Liu；J. Liu；A. Vasileff；Y. Jiao；Y. Zheng；S.-Z. Qiao. Emerging Two-Dimensional Nanomaterials for Electrocatalysis. *Chemical Reviews*. **2018**, *118*, 6337-6408.

(8). A. Thomas. Functional materials: from hard to soft porous frameworks. *Angew Chem Int Ed Engl*. **2010**, *49*, 8328-8344.

(9). P. J. Waller；F. Gándara；O. M. Yaghi. Chemistry of Covalent Organic Frameworks. *Accounts of Chemical Research*. **2015**, *48*, 3053-3063.

(10). J. Zhang；Y. Chen；X. Wang. Two-dimensional covalent carbon nitride nanosheets: synthesis, functionalization, and applications. *Energy & Environmental Science*. **2015**, *8*, 3092-3108.

(11). Z. Zhang；N. Han；L. Tan；Y. Qian；H. Zhang；M. Wang；W. Li；Z. Cui；X. Zhang. Bioinspired Superwettable Covalent Organic Framework Nanofibrous Composite Membrane with a Spindle-Knotted Structure for Highly Efficient Oil/Water Emulsion Separation. *Langmuir*. **2019**, *35*, 16545-16554.

(12). Y. Jiang；C. Liu；Y. Li；A. Huang. Stainless-steel-net-supported superhydrophobic COF coating for oil/water separation. *Journal of Membrane Science*. **2019**, *587*,

(13). B. P. Biswal；H. D. Chaudhari；R. Banerjee；U. K. Kharul. Chemically Stable Covalent Organic Framework (COF)-Polybenzimidazole Hybrid Membranes: Enhanced Gas Separation through Pore Modulation. *Chemistry - A European Journal*. **2016**, *22*, 4695-4699.

(14). W. Li；C.-X. Yang；X.-P. Yan. A versatile covalent organic framework-based platform for sensing biomolecules. *Chem. Commun.* **2017**, *53*, 11469-11471.

(15). Y. Lu；J. He；Y. Chen；H. Wang；Y. Zhao；Y. Han；Y. Ding. Effective Acetylene/Ethylene Separation at Ambient Conditions by a Pigment-Based Covalent-Triazine Framework. *Macromolecular Rapid Communications*. **2018**, *39*,

(16). H.-L. Qian；C.-X. Yang；W.-L. Wang；C. Yang；X.-P. Yan. Advances in covalent

organic frameworks in separation science. *Journal of Chromatography A*. **2018**, *1542*, 1-18.

(17). H.-L. Qian；C. Yang；X.-P. Yan. Layer-by-layer preparation of 3D covalent organic framework/silica composites for chromatographic separation of position isomers. *Chemical Communications*. **2018**, *54*, 11765-11768.

(18). Y. Wang；S. Zhuo；J. Hou；W. Li；Y. Ji. Construction of β-Cyclodextrin Covalent Organic Framework-Modified Chiral Stationary Phase for Chiral Separation. *ACS Applied Materials & Interfaces*. **2019**, *11*, 48363-48369.

(19). J. Sun；A. Klechikov；C. Moise；M. Prodana；M. Enachescu；A. V. Talyzin. A Molecular Pillar Approach To Grow Vertical Covalent Organic Framework Nanosheets on Graphene: Hybrid Materials for Energy Storage. *Angew Chem Int Ed Engl*. **2018**, *57*, 1034-1038.

(20). Y. Tang；S. Feng；L. Fan；J. Pang；W. Fan；G. Kong；Z. Kang；D. Sun. Covalent organic frameworks combined with graphene oxide to fabricate membranes for H2/CO2 separation. *Separation and Purification Technology*. **2019**, *223*, 10-16.

(21). P. Wang；Q. Wu；L. Han；S. Wang；S. Fang；Z. Zhang；S. Sun. Synthesis of conjugated covalent organic frameworks/graphene composite for supercapacitor electrodes. *RSC Advances*. **2015**, *5*, 27290-27294.

(22). A. K. Geim. Graphene: Status and Prospects. *Science*. **2009**, *324*, 1530-1534.

(23). A. K. Geim；K. S. Novoselov. The rise of graphene. *Nat Mater*. **2007**, *6*, 183-191.

(24). K. S. Novoselov. Electric Field Effect in Atomically Thin Carbon Films. *Science*.

2004, *306*, 666-669.

(25). M. Hu；B. Mi. Enabling Graphene Oxide Nanosheets as Water Separation Membranes. *Environmental Science & Technology*. **2013**, *47*, 3715-3723.

(26). W.-S. Hung；C.-H. Tsou；M. De Guzman；Q.-F. An；Y.-L. Liu；Y.-M. Zhang；C.-C. Hu；K.-R. Lee；J.-Y. Lai. Cross-Linking with Diamine Monomers To Prepare Composite Graphene Oxide-Framework Membranes with Varying d-Spacing. *Chemistry of Materials*. **2014**, *26*, 2983-2990.

(27). P. Sun；K. Wang；H. Zhu. Recent Developments in Graphene-Based Membranes: Structure, Mass-Transport Mechanism and Potential Applications. *Advanced Materials*. **2016**, *28*, 2287-2310.

(28). Z. Wang；Y. Li；P. Liu；Q. Qi；F. Zhang；G. Lu；X. Zhao；X. Huang. Few layer covalent organic frameworks with graphene sheets as cathode materials for lithium-ion batteries. *Nanoscale*. **2019**, *11*, 5330-5335.

(29). Y. Ying；D. Liu；J. Ma；M. Tong；W. Zhang；H. Huang；Q. Yang；C. Zhong. A GO-assisted method for the preparation of ultrathin covalent organic framework membranes for gas separation. *Journal of Materials Chemistry A*. **2016**, *4*, 13444-13449.

(30). N. A. Khan；J. Yuan；H. Wu；L. Cao；R. Zhang；Y. Liu；L. Li；A. U. Rahman；R. Kasher；Z. Jiang. Mixed Nanosheet Membranes Assembled from Chemically Grafted Graphene Oxide and Covalent Organic Frameworks for Ultra-high Water Flux. *ACS Applied Materials & Interfaces*. **2019**, *11*, 28978-28986.

(31). X. Zhang；H. Li；J. Wang；D. Peng；J. Liu；Y. Zhang. In-situ grown covalent

organic framework nanosheets on graphene for membrane-based dye/salt separation. *Journal of Membrane Science*. **2019**, *581*, 321-330.

(32). Y. Liu；J. Guan；Y. Su；R. Zhang；J. Cao；M. He；J. Yuan；F. Wang；X. You；Z. Jiang. Graphene oxide membranes with an ultra-large interlayer distance through vertically grown covalent organic framework nanosheets. *Journal of Materials Chemistry A*. **2019**, *7*, 25458-25466.

(33). D. Mullangi；V. Dhavale；S. Shalini；S. Nandi；S. Collins；T. Woo；S. Kurungot；R. Vaidhyanathan. Low-Overpotential Electrocatalytic Water Splitting with Noble-Metal-Free Nanoparticles Supported in a sp3N-Rich Flexible COF. *Advanced Energy Materials*. **2016**, *6*,

(34). S. Navalón；J. R. Herance；M. Álvaro；H. García. General aspects in the use of graphenes in catalysis. *Materials Horizons*. **2018**, *5*, 363-378.

(35). S. Sabater；J. A. Mata；E. Peris. Catalyst Enhancement and Recyclability by Immobilization of Metal Complexes onto Graphene Surface by Noncovalent Interactions. *ACS Catalysis*. **2014**, *4*, 2038-2047.

(36). K. M. Yam；N. Guo；Z. Jiang；S. Li；C. Zhang. Graphene-Based Heterogeneous Catalysis: Role of Graphene. *Catalysts*. **2020**, *10*,

(37). M. Su；Y. Liu；S. Li；Z. Fang；B. He；Y. Zhang；Y. Li；P. He. A rubber-like, underwater superoleophobic hydrogel for efficient oil/water separation. *Chemical Engineering Journal*. **2019**, *361*, 364-372.

(38). X. Zhang；J. Zhao；L. Ma；X. Shi；L. Li. Biomimetic preparation of a polycaprolactone membrane with a hierarchical structure as a highly efficient oil–

water separator. *Journal of Materials Chemistry A*. **2019**, *7*, 24532-24542.

(39). J. Liu；L. Wang；N. Wang；F. Guo；L. Hou；Y. Chen；J. Liu；Y. Zhao；L. Jiang. A Robust Cu(OH)2Nanoneedles Mesh with Tunable Wettability for Nonaqueous Multiphase Liquid Separation. *Small*. **2017**, *13*,

(40). M. Zhang；B. Guo；Y. Feng；C. Xie；X. Han；X. Kong；B. Xu；L. Zhang. Amphipathic Pentiptycene-Based Water-Resistant Cu-MOF for Efficient Oil/Water Separation. *Inorganic Chemistry*. **2019**, *58*, 5384-5387.

(41). J.-C. Wang；H. Lou；Z.-H. Cui；Y. Hou；Y. Li；Y. Zhang；K. Jiang；W. Shi；L. Qu. Fabrication of porous polyacrylamide/polystyrene fibrous membranes for efficient oil-water separation. *Separation and Purification Technology*. **2019**, *222*, 278-283.

(42). X. Du；L. Fan；M. Zhang；Z. Kang；W. Fan；M. Wen；Y. Zhang；M. Li；R. Wang；D. Sun. Surface wettability switching of a zeolitic imidazolate framework mesh via surface ligand exchange for oil-water separation. *Materials Research Bulletin*. **2019**, *111*, 301-305.

(43). T.-h. Zhang；T. Yan；G.-q. Zhao；W. Hu；F.-p. Jiao. Superhydrophobic micro/nanostructured copper mesh with self-cleaning property for effective oil/water separation. *Chinese Journal of Chemical Physics*. **2019**, *32*, 635-642.

(44). Y. Yang；Z. Guo；W. Huang；S. Zhang；J. Huang；H. Yang；Y. Zhou；W. Xu；S. Gu. Fabrication of multifunctional textiles with durable antibacterial property and efficient oil-water separation via in situ growth of zeolitic imidazolate framework-8 (ZIF-8) on cotton fabric. *Applied Surface Science*. **2020**, *503*,

(45). X. Miao；L. Han；L. Wang；M. Wang；X. Sun；X. Zhu；B. Ge. Preparation of PDVB/TiO2 composites and the study on the oil-water separation and degradation performances. *Science China Technological Sciences*. **2019**, *62*, 1217-1223.

(46). X. Wang；Y. Pan；H. Yuan；M. Su；C. Shao；C. Liu；Z. Guo；C. Shen；X. Liu. Simple fabrication of superhydrophobic PLA with honeycomb-like structures for high-efficiency oil-water separation. *Chinese Chemical Letters*. **2020**, *31*, 365-368.

Figure captions

Figure 1. (a) Schematic showing the one-step fabrication method for COF/GO$_x$ composition followed by membrane preparation via spraying the composite onto the filter paper. And (b) the growth mechanism of COF on the GO sheets at the molecular level and the role of grapheme oxide as Schiff base carrier.

Figure 2. (a) SEM image of GO. (b) SEM image of COF/GO$_{50}$. (c) - (e) TEM images of COF/GO$_{50}$. (f) - (g) EDS mapping of COF particles.

Figure 3. (a) FTIR spectra of GO, GO and COF/GO$_{50}$. (b) - (c) C 1s XPS of GO and COF/GO$_{50}$, respectively.

Figure 4. Physicochemical characterization of COF/GO (a) TGA analysis curves of COF/GO$_x$ and GO. (b) XRD pattern of COF/GO$_{50}$. (c) Nitrogen adsorption-desorption curves of COF/GO$_{50}$ and GO. (d) Pore size distribution of COF/GO$_{50}$ and GO.

Figure 5. (a)WCAs of water with acidic (pH=1) and basic (pH=13) pH on GO membrane. (b) Images of toluene and chloroform drops on the COF/GO$_{50}$ membrane showing complete wettability. (c) Change in the WCSs with GO proportions in COF/GO membranes. (d) WCAs on COF/GO$_{50}$ membrane with different acidic and basic pH. The droplets were placed for ~2 minutes and no change in the angles have been recorded.

Figure 6. Separation performance of COF/GO$_{50}$ membrane (a) Flux and separation efficiency of four types water/oil mixtures. (b) Flux and separation efficiency during 20 repeated cycles of water/dichloromethane mixture.

Figure 7. Separation performance of COF/GO$_{50}$ membrane under adverse conditions

(a) Flux and separation efficiency of different pH water/oil mixtures. (b) Flux and separation efficiency during 20 cycles of water (pH=1)/n-hexane mixture. (c) Flux and separation efficiency during 20 cycles of water (pH=13)/n-hexane mixture.

Table of contents: